applied sciences

MDPI

Article

Influence of the Polarity of the Electric Field on Electrorheometry

J. Hermenegildo García-Ortiz [1], Samir H. Sadek [2] and Francisco J. Galindo-Rosales [3,*]

1 Departamento de Ingeniería Mecánica y Diseño Industrial, Escuela Superior de Ingeniería, Universidad de Cádiz, Av. Universidad de Cádiz, 10, Puerto Real, 11519 Cádiz, Spain; mere.garcia@uca.es
2 Departamento de Engenharia Mecânica, Centro de Estudos de Fenómenos de Transporte (CEFT), Faculdade de Engenharia da universidade do Porto, Rua Dr. Roberto Frias s/n, CP4200-465 Porto, Portugal; sadek@gcloud.fe.up.pt
3 Departamento de Engenharia Química, Centro de Estudos de Fenómenos de Transporte (CEFT), Faculdade de Engenharia da universidade do Porto, Rua Dr. Roberto Frias s/n, CP4200-465 Porto, Portugal
* Correspondence: galindo@fe.up.pt or curro@galindorosales.com

Received: 5 November 2019; Accepted: 25 November 2019; Published: 4 December 2019

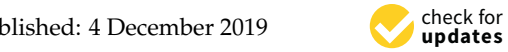

Abstract: Uniaxial extensional flow is a canonical flow typically used in rheological characterization to provide complementary information to that obtained by imposing simple shear flow. In spite of the importance of having a full rheological characterization of complex fluids, publications on the rheological characterization of mobile liquids under extensional flow have increased significantly only in the last 20 years. In the case of the rheological characterization of electrorheological fluids, the situation is even more dramatic, as the ERFs have been exclusively determined under simple shear flow, where an electrorheological cell is attached to the rotational rheometer generating an electric field perpendicular to the flow direction and that does not allow for inverting the polarity. The very recent work published by Sadek et al., who developed a new electrorheological cell to be used with the commercial Capillary Breakup Extensional Rheometer (CaBER), allows for the very first time performing electrorheometry under extensional flow. By means of the same experimental setup, this study investigates the influence of the polarity of the imposed electric field on the filament thinning process of a Newtonian and an electrorheological fluid. Results show that a polarity against the gravity results in filament thinning processes that live longer or reach a stable configuration at lower intensities of the applied electric field.

Keywords: electrorheology; extensional flow; capillary breakup extensional electrorheometry (CaBEER); dielectric liquid bridge

1. Introduction

More than eighty years ago, W.M. Winslow reported that some suspensions of non-conducting, but electrically active particles dispersed in an electrically insulating fluid exhibit a reversible sudden increase of the viscosity under the application of an external electric field [1,2]. Still, currently, this phenomenon remains known as the Winslow effect, but it is also known as the electrorheological effect. Electrorheology is, therefore, a branch of rheology dealing with the study and characterization of the rheological properties of electro-responsive materials [3].

In order to model electrorheological fluids (ERFs) accurately, detect subtle dissimilarities in their composition, and describe or predict the processing conditions that will optimize the fluid flow or characteristics of the final product, a thorough rheological characterization of these materials in both shear and extensional flow conditions is recommended [4]. Among the plethora of techniques to perform a rheological characterization with commercial rheometers [5], the ERFs have been

traditionally studied by means of rotational rheometers, which are devices that impose either a torque or a velocity of rotation and measure the response in terms of angular deformation or torque, respectively. An electrorheological cell imposes the external electric field to the fluid sample, which is perpendicular to the flow field generated in the fluid by the rotational rheometer. It is widely accepted that, after a few milliseconds of the application of an external electric field, the suspended particles form chains along the direction of the electric field [6–8]. Based on this model, it can be concluded that under shear flow with an electric field perpendicular to the flow direction, the particle chains undergo a shearing force. In an attempt to characterize the effect of a force aligned with the particle chain, ERFs have also been characterized in squeeze flow by means of a rotational rheometry [9]; however, there are important issues with these kinds of experiments, such as the lack of accuracy in determining the real slip condition, the compliance of the instrument, and the fact that the shear wall effect makes it impossible to analyze the pure extensional behavior of the ERFs [10,11]. To the best of the authors knowledge, the electrorheological cells designed for rotational rheometers do not allow changing the polarity in the electric field, and therefore, the influence of the polarity in the shear characterization of the ERFs has not been reported yet.

In order to characterize the extensional properties of complex fluids properly, it is recommended to impose a uniaxial extensional flow. Nevertheless, due to technical challenges, there is no special add-on for rotational rheometers allowing the extensional characterization of liquid-like fluids. For the extensional characterization of fairly mobile liquids there are currently two commercial devices available, i.e., FiSER and CaBER, but none of them are equipped with an electrorheological cell allowing the application of an external electric field [12]. Very recently, Sadek et al. [13] developed an add-on, named the Extensional Electrorheological Fixture (ExERF) [13], that overcomes this limitation for the CaBER device and allows performing Capillary Breakup Extensional Electrorheometry (CaBEER) [14]. This pioneering work allows the characterization of ERFs under the simultaneous application of an electrical field and an extensional flow both aligned with gravity; however, the influence of the polarity of the electric field in the measurements has not been reported yet.

In this study, we focus our attention on the influence of the polarity on the rheological behavior of ERFs and its suspending fluid under shear and extensional flow conditions. It has been found that the polarity of the electric field indeed affects the filament thinning process of both the carrier fluid (olive oil) and the electrorheological fluid. The general idea is that the electric field, when oriented in the opposite direction of gravity, generates Coulombian forces that counterbalance the gravitational force. This conclusion and other results that can be obtained by means of CaBEER with different liquids may have a relevant impact on the study of the stability and dynamics of liquid bridges under the presence of an external electric field, which may open new doors for pioneering works in a broad range of applications, including crystal growth, surface patterning, nano-printing, nano-lithography, aggregation and coalescence of flexible fibers, and capillary induced collapse of elastic structures [15].

2. Materials and Methods

2.1. Fluids

The working fluids consisted of suspensions of cornstarch (Maizena, Unilever Jerónimo Martins, Lda) in commercial extra virgin olive oil (Table 1) at concentrations of 0 and 30 wt.%. The protocol for the preparation of the samples was the same described by Sadek et al. [13]. Before use, the samples were re-dispersed in an ultrasound bath (Velleman VTUSC3).

Table 1. Chemical characteristics of the commercial extra virgin olive oil.

Property	Value
Free Fatty Acidity (FFA) (%)	$\leq$0.8
Long Chain Fatty Acids (waxes) (mg/kg)	$\leq$150
Peroxides (mEqO_2/kg)	$\leq$20

The size and volumetric distribution of the cornstarch particles were determined by means of low angle front light scattering measurements (LS230 Laser Diffraction Particle Size Analyzer, Beckman Coulter Inc., Brea, California, United States). The results are shown in Figure 1b, and two peaks can be observed at 1.3 µm and 14.3 µm. In addition, the bright field microscopy performed on an inverted microscope (DMI 5000M, Leica Microsystems GmbH, Wetzlar, Germany) with a monochromatic CCD camera sensitivity sensor (DFC350 FX, Leica Microsystems GmbH, Wetzlar, Germany) and a 10× objective lens (Leica HCX PL Fluotar L CORR, numerical aperture (NA) = 0.40) confirmed the bimodal particle size distribution of the cornstarch.

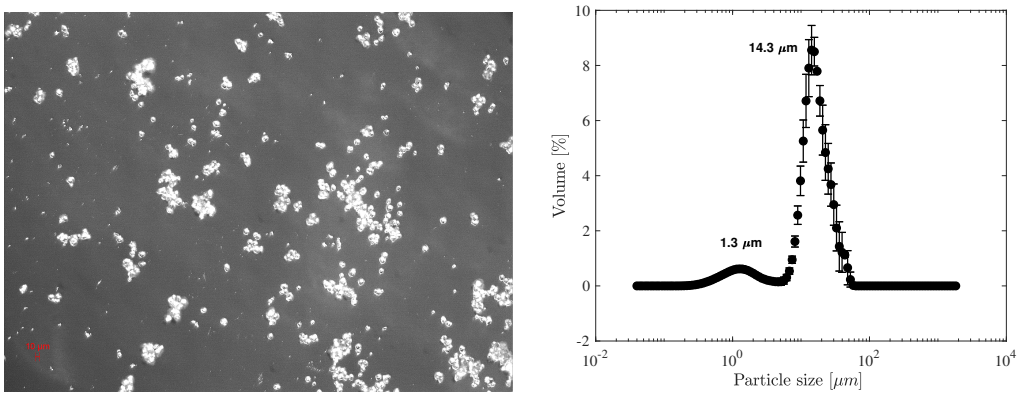

(a) **(b)**

Figure 1. (**a**) Bright field microscope image of the cornstarch and (**b**) particle size distribution, where the error bars represent the standard deviation of three independent measurements (reprinted with permission from Sadek et al. Journal of Rheology 64, 43 (2020) [14], Copyright 2020, The Society of Rheology).

The surface tension (σ) and the density (ρ) of the working fluids are shown in Table 2. The density was measured using a 25 mL pycnometer. The surface tension was measured by means of the Sigma 700 force tensiometer (Biolin Scientific, Gothenburg, Sweden), equipped with a Du Noüy ring method with a ring 9.58 mm in diameter and 0.185 mm in thickness. Both experiments were performed at room temperature (20 °C).

Table 2. Fluid properties of cornstarch/olive suspension of different concentrations at 20 °C.

Property	0 wt.%	30 wt.%
ρ (kg/m^3)	917	1076
σ (mN· m)	∼32	∼32

2.2. Rheometry

2.2.1. Simple Shear Flow

The rheological characterization under simple shear flow was carried out in a stress controlled rotational rheometer (Anton Paar MCR301), which was equipped with an electrorheological device (ERD) and concentric cylinders. The outer cylinder was fixed, while the inner cylinder rotated and imposed a shear stress (τ) at its wall. The rotating cylinder had a radius of $R_i = 13.33$ mm and a length of 39.97 mm, while the radius of the cup was $R_e = 19.99$ mm. The electrorheological cell applied an electric field ($\vec{E} = \frac{\Delta V}{R_e - R_i}\vec{e_r}$) in the radial direction, where ΔV is the applied potential difference. Thus, the electric field and the velocity field were perpendicularly oriented (Figure 2a). It is worth mentioning that it is not possible to change the polarity in the ERD connected to the rotational rheometer. The temperature within the sample fluid was fixed at 20 °C with a Peltier temperature controller.

It is widely accepted that electrorheological fluids exhibit yield stress under the presence of an electric field, and their flow behavior is reasonably well modeled by the Bingham model (Equation (1)):

$$\tau = \tau_{yd} + \eta_p \dot{\gamma}, \tag{1}$$

where η_p is the plastic viscosity, $\dot{\gamma}$ is the shear rate, and τ_{yd} is the dynamic yield stress. The dynamic yield stress can be measured by extrapolating to zero shear rate the steady-state flow curve obtained with a decreasing ramp in shear stress (1000–0.01 Pa) [16]. The steady-shear flow curves were determined for both fluids at different electric field values (0, 0.5, 0.75, 1, 1.5, 2.25, 3 kV/mm).

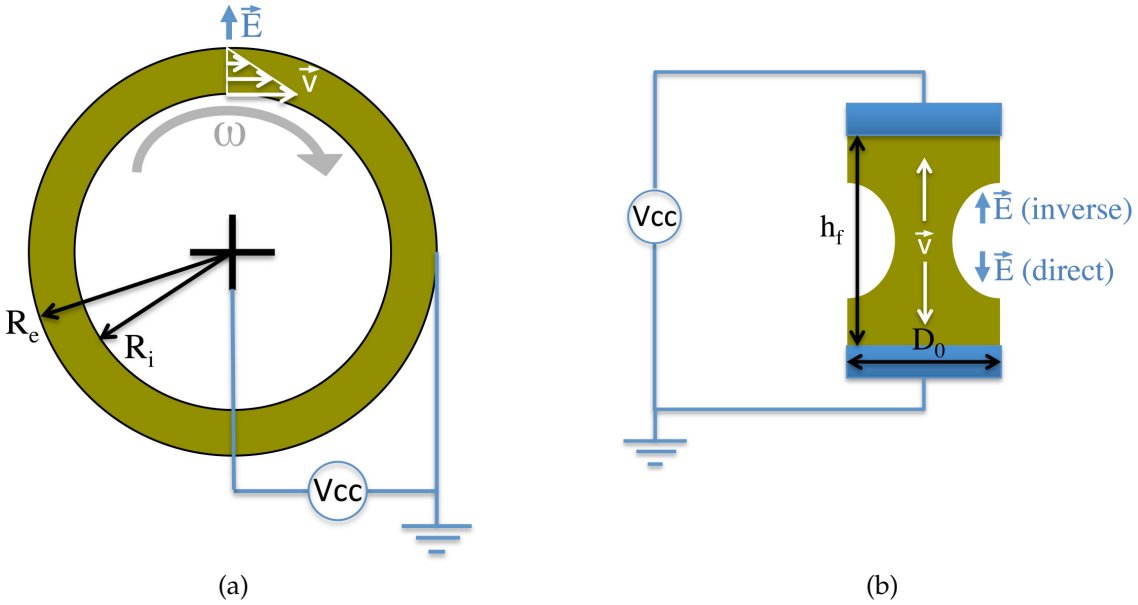

Figure 2. (**a**) Sketch of the rotational rheometer equipped with an electrorheological cell and concentric cylinders (top view), where the electric and velocity fields are perpendicularly oriented. (**b**) Sketch of the CaBER device equipped with the electrorheological cell (front view), where the electric and velocity fields are parallel to each other, independent of the polarity.

2.2.2. Capillary Breakup Extensional Electrorheometry

Capillary breakup extensional electrorheometry experiments were carried out in a CaBER device (Thermo Fisher Scientific, Waltham, MA, USA) equipped with the Extensional Electrorheological Fixture (ExERF) [13]. The CaBER imposes a step strain extensional deformation (from h_0 to h_f) to a stable liquid bridge, reaching a non-equilibrium state from which the capillary forces trigger the thinning process of the filament until it breaks. From the time evolution of the filament thinning process, it is possible to characterize the extensional behavior of the fluids [17,18]. The ExERF generates a potential difference between the plates, limited to the maximum voltage generated by a high voltage sequencer (HVS448 3000V, LabSmith, Inc., Livermore, CA, USA). The desired electric field is given by $\vec{E} = \Delta V / h_0$, ΔV being the potential difference and h_0 the initial gap, which was set at 2 mm for all the experiments. If the field goes from the upper to the lower plate, it is denoted as direct polarity; on the other hand, if the field goes from the lower to the top plate, it is denoted as inverse polarity (Figure 2b). The electric fields, which are aligned with the extensional flow, were set at: 0, 0.5, 0.75, 0.9, 1, 1.125, 1.25, and 1.5 kV/mm. The final height of the liquid bridge (h_f) was set to 6 mm for all cases studied. At least three independent runs were performed in order to ensure the reproducibility of the results presented below.

These values provided a Hencky strain value $\epsilon = ln\left(\frac{h_f}{h_0}\right) = 1.10$. The optimal value of $\Lambda_0 = \frac{h_0}{d_0}$ is in the range of $0.5 \leq \Lambda_0 \leq 1$, as indicated by the data from Yao and McKinley [19]. In this study,

4 mm diameter plates were used, and Λ_0 was set at 0.5 due to the low value of the surface tension of the working fluids. Finally, the initial stretch profile was linear with a streak time t_s = 20 ms, and the temperature control was set to 20 °C (Thermo Haake DC10). The initial and final heights were checked regularly with thickness gauges, while the temperature of the fluid was measured before and after the experiments with a thermocouple sensor, which confirmed that the fluid temperature was not increased due to the Joule heating effect occurring during the lifetime of the experiments. As the fluid sample was based on olive oil, which had a conductivity close to 0 μS, the intensity of the current (I) through the liquid bridge was extremely low, resulting in a negligible power of heating ($P \propto R^2$) generated during the experiments. If the sample were conductive, the Joule heating effect would increase the temperature of the sample during the experiment, resulting in a decrease in the viscosity of the sample with time, which would make it impossible to decouple the effect of the polarity from the effect of the variation in the viscosity. The filament thinning process was recorded exclusively by means of a high-speed video camera (Photron FASTCAM Mini UX100) at 3200 fps (1024 × 1280 square pixel) because for non-cylindrical filaments, the breaking is not fixed in the center of the filament and can be out of laser range [20–22]. The high speed camera was equipped with a set of optical lenses (Optem Zoom 70 XL) with 2× magnification. A 52 mm Telecentric Backlight Illuminator connected to a metal halide light source (LeicaEL6000) by an optical fiber cable was used to illuminate the liquid bridge with truly collimated light and produce high contrast, silhouetted images. All the components of the experimental setup are indicated in Figure 3.

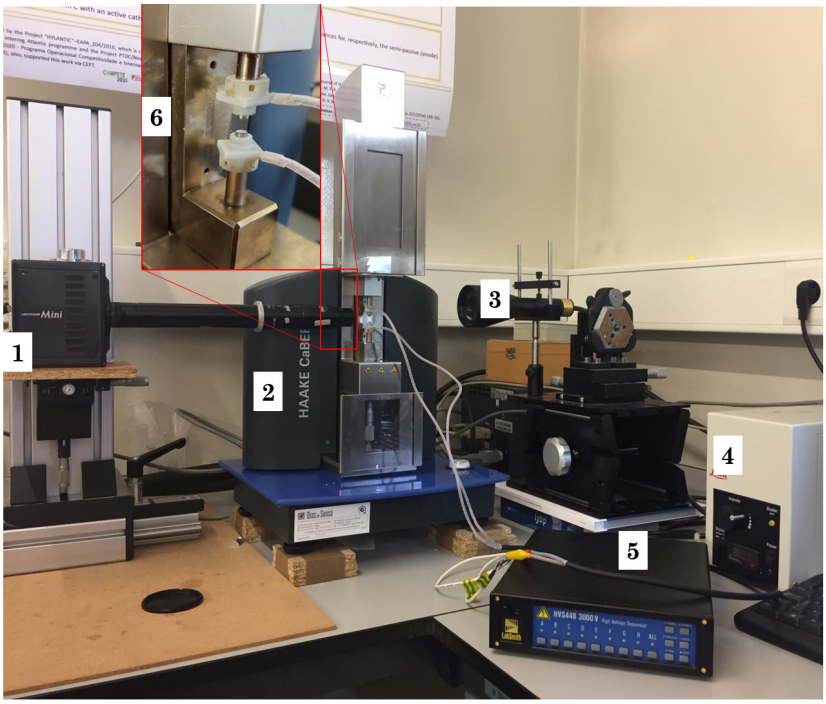

Figure 3. Experimental setup: (1) high speed camera, (2) CaBER device, (3) Telecentric Backlight Illuminator, (4) light source, (5) voltage generator, and (6) ExERF ([13]).

In the experimental procedure, the fluid was first loaded between the plates, which were separated by the initial height h_0. Then, the voltage was applied (corresponding to an electric field of $E_0 = \Delta V/h_0$), and the CaBER was ordered, without delay, to trigger the step strain deformation. Najafabadi et al. [23] showed that the delay between applying the electric field and triggering the experiment plays an important role in CaBEER results. The difference in density between the particles ($\rho = 1600$ kg/m^3) and the carrier fluid ($\rho = 917$ kg/m^3) can be a problem in the CaBER experiment. From the Stokes equation, the sedimentation time taken by a particle to move from the midpoint of the filament ($h_0/2$) to the bottom plate was 275 s. Once the sample was loaded, the field was immediately imposed,

the stretch profile was imposed (maximum delay smaller than 5 s), and the thinning process of the filament was recorded. The whole process, from loading the sample until the end of the thinning, lasted less than 10 s. Therefore, the sedimentation time was more than 20 times the duration of the experiment, and the dispersion could be considered stable enough for the characteristic time of the CaBEER experiments, with the possibility of the appearance of a particle gradient in the sample being ruled out before starting the experiment.

Another relevant aspect to consider is the relationship between field strength and the thermal fluctuations of the particles. This ratio was studied by Gast and Zukoski [6], who defined a dimensionless parameter $\lambda = \frac{\pi\epsilon_0\epsilon_c a^3\beta^2 E_0^2}{2kT}$, where ϵ_0 is the permittivity of free space, a the particle diameter, ϵ_c the relative dielectric constant of the continuous phase [24], $\beta = \frac{\sigma_p - \sigma_c}{\sigma_p + 2\sigma_c}$(dc field), σ_p and σ_c are the electrical conductivities of the particulate and the continuous phases [25], E_0 the applied electric field strength, k the Boltzmann constant, and T the absolute temperature. Hence, if $\lambda \gg 1$, strong electric interactions are identified, while if $\lambda \ll 1$, the Brownian motion dominates. For the experimental conditions and the working fluids considered in this study, it could be confirmed that $\lambda \gg 1$, which was representative of a structure possessing sizeable yield stress and typical shear viscosity orders of magnitude larger than that of the solvent at low shear rates.

3. Results and Discussion

3.1. Newtonian Fluid

Extra virgin olive oil was the suspending fluid, and it exhibited a Newtonian behavior. It was measured both under shear and extensional flows, with and without the application of the electric field, obtaining different results.

Figure 4 shows the steady-state deformation with the stress of the olive oil measured in the rotational rheometer at 20 °C with and without the influence of an electric field. It can be observed that all the curves overlapped, which was clear evidence for the presence of the electric field, and its intensity did not affect the rheological behavior of the olive oil under shear flow. As mentioned above, the electrorheological cell in the rotational rheometer did not allow changing the polarity in the electric field, which was perpendicularly oriented to the flow field. In the absence of particles, the electric field had no possibility to build any structure in the olive oil, and the viscosity did not change with E_0.

Figure 5 shows the time evolution of the minimum filament diameter once the fluid bridge reached the final position $h_f = 6$ mm. It can be observed that the presence of the imposed electric field E_0 slightly modified the curve measured without the presence of the electric field. The influence of the polarity imposed on that change could also be appreciated; the filament lived longer when the electric field was pointing upward (inverse polarity), while its breakup time became shorter when the polarity was oriented with the direction of gravity (direct polarity).

Additionally, at h_0, once the field was applied, a slight vibration of the liquid–air interface (Video S1 in the Supplementary Material) was observed, which was modified. Figure 6a shows that the polarity of the electric field had an effect on the minimum diameter of the liquid bridge. Figure 6b shows the silhouette of the liquid bridges before applying the voltage and after 8.5 s of the application of the voltage. It can be observed that the inverse polarity helped to keep the shape of the filament unchanged ($\Delta D_0^{Inv} = \frac{\Delta(R/R_0)}{\Delta t} = 0.0124$), while the direct polarity led to a more intense decrease in the diameter ($\Delta D_0^{Dir} = \frac{\Delta(R/R_0)}{\Delta t} = 0.0308$). Moreover, it can be observed that in the case of the direct polarity, the vertical position of the minimum diameter moved down. These results confirmed that the direct polarity had a similar effect to having a larger Bond number, which would lead to shorter break up times in the filament.

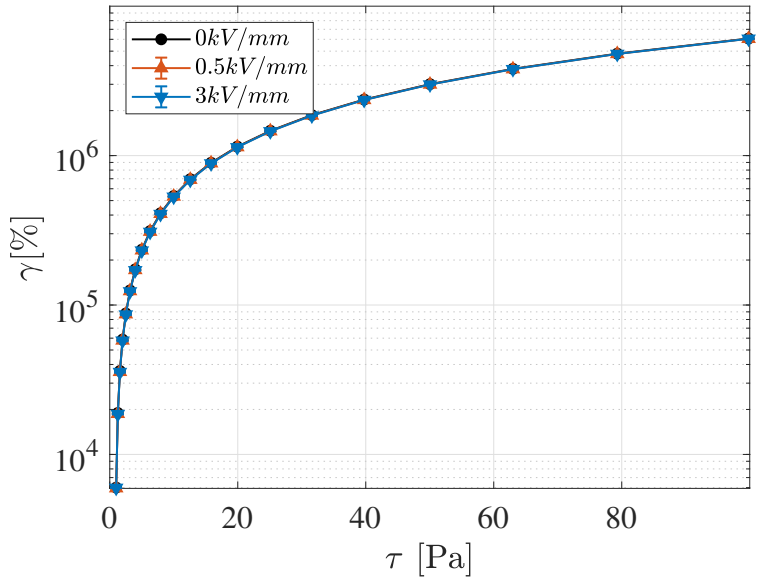

Figure 4. Viscosity curve of the olive oil measured in the rotational rheometer at 20 °C with and without the influence of an electric field.

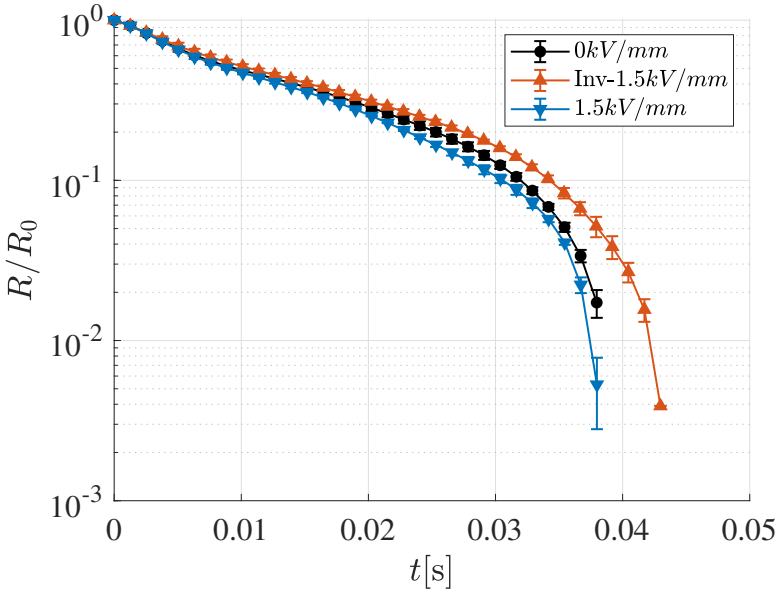

Figure 5. Time evolution of the normalized diameter for the Newtonian fluid. Influence of the presence of the electric field and its polarity.

According to González et al. [26], the electrical currents are very small in a highly insulating liquid bridge, and then, the electrical forces ($\vec{F_{V,e}}$) participating in the problem would be the following ones:

- Coulombian-type forces ($\rho_e \vec{E}$), which are due to the presence of the free charge density (ρ_e) that probably comes from the dissociation of impurities or of the liquid itself, apart from the inevitable electrochemical reactions at the metal–electrode/liquid interface. The dynamics of the liquid will be strongly affected by this type of force in a DC electric field.
- Dielectrophoretic force ($\frac{1}{2}E^2\nabla\epsilon$), which results from the inhomogeneity in the electrical permittivity (ϵ) when the fluid undergoes electrical stress, acts at the air–liquid interface and perpendicularly to it. Therefore, it is not a volume force.

- Electrostrictive force ($\frac{1}{2}\nabla\left[\rho\left(\frac{d\epsilon}{d\rho}\right)_T E^2\right]$), which acts both at the interface and on the liquid bulk, is irrelevant to the dynamics of the liquid, and the usual convention neglects its contribution.

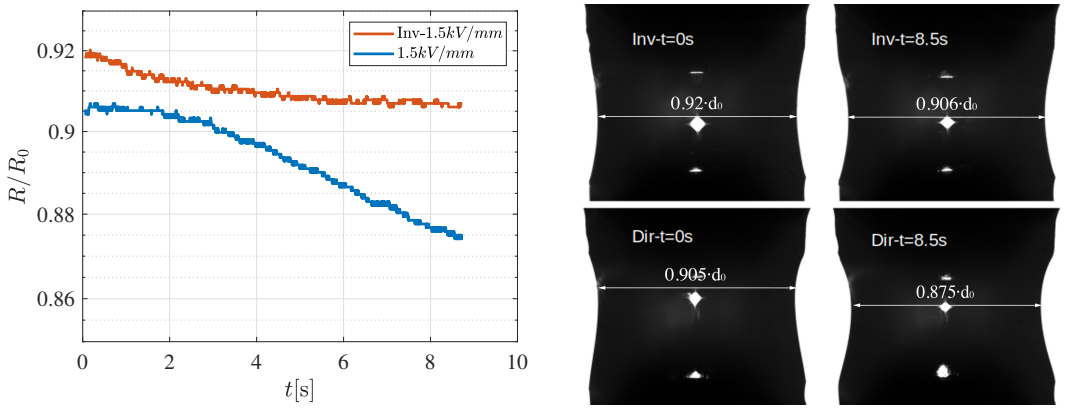

Figure 6. (**a**) Time evolution of the minimum radius for the Newtonian fluid at h_0; no step strain was applied, just the electric field. (**b**) First ($t = 0$ s) and last image ($t = 8.5$ s) of the liquid bridging the initial height for the different polarity: top row for inverse (Supplementary Material, Video S1) and bottom row for direct (Supplementary Material, Video S2).

Thus, the differences in the filament thinning process of the Newtonian fluid due to the polarity can be explained due to the direction of the Coulombian-type force. In the case of the direct polarity, it would have a similar effect as having a higher bond number, and the breakup time of the filament would be shorter; while in the case of the inverse polarity, the Coulombian force would counterbalance the gravity force, and the filament would live longer.

3.2. Cornstarch/Oil Suspension

3.2.1. Shear Electrorheometry

Figure 7a shows the viscosity curves of the working fluids measured under steady-shear flow, following the experimental protocol detailed in Section 2.2.1. It is worth highlighting that the curve of the ERF without the influence of the electric field is parallel to the one of the carrying fluid. This result means that the ERF exhibited a Newtonian-like behavior under shear flow without the presence of the electric field, but with a viscosity slightly larger than that of the carrying fluid due to the presence of the suspended particles. Figure 7a also shows that the viscosity of the ERF increased by increasing the intensity of the imposed electrical field. The ERFs can be modeled reasonably well by the Bingham plastic model (Equation (2)), from which the dynamic yield stress value, τ_{yd}, can be obtained by extrapolating the experimental curves until $\dot{\gamma} = 0$:

$$\tau = \eta_p \dot{\gamma} + \tau_{yd} \tag{2}$$

where τ is the shear stress, η_p is the plastic viscosity, and $\dot{\gamma}$ is the shear rate. The dependence of the dynamic yield stress with the applied electric field (E_0) is given by a power law function ($\tau_{yd} = A \cdot E_0^B$), whose fitting parameters are shown in Table 3 for the ERF considered in this study. It has been widely accepted in the literature [8,27] that $\tau_{yd} \propto E_0^2$; however, the electric field exponents $B's$ in our cases were significantly lower due to water content, which is consistent with the results reported in the literature by Davis et al. [28] and Li and Chen [25].

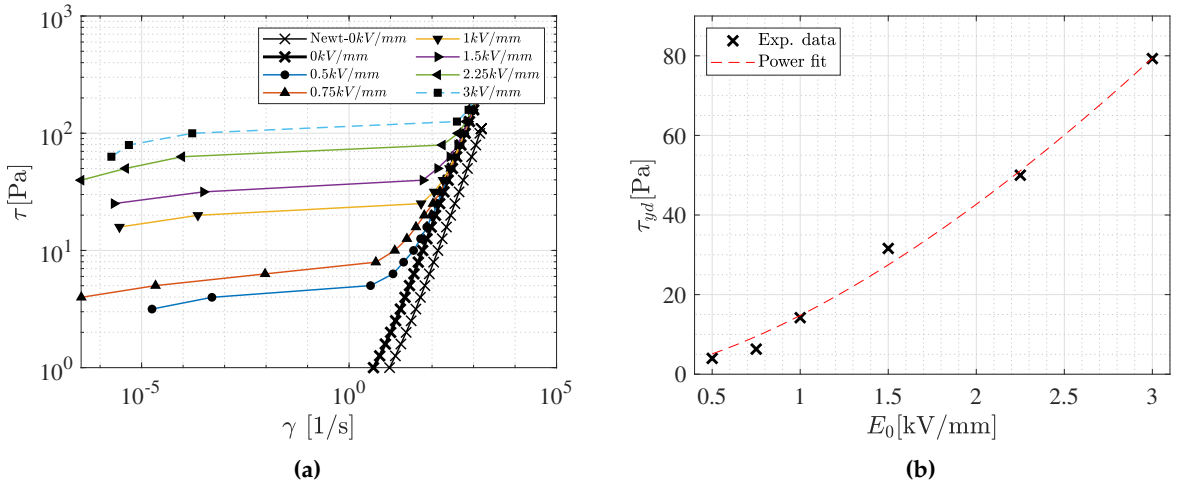

(a) **(b)**

Figure 7. (**a**) Steady-state viscosity curves for the suspending fluid and the ERF under an imposed electrical field of 0, 0.5, 0.75, 1, 1.5, 2.25, and 3 kV/mm. (**b**) Dependence of the dynamic yield stress with the intensity of the electric field imposed at h_0.

Table 3. Dependence of the dynamic yield stress with the applied electric field ($\tau_{yd}(E_0) = A \cdot E_0^B$, with E_0 in kV/mm) for the cornstarch/olive suspension.

Fitting Parameters	*A*	*B*	R^2
30 wt.%	14.7	1.54	0.983

3.2.2. Extensional Electrorheometry

Shear electrorheometry measurements allowed confirming that the ERF exhibited a Newtonian-like behavior when no electrical field was applied, but a yield stress behavior under the presence of an electrical field. The ERF showed a potential dependence of the yield stress value with the applied electric field. Once the shear sample was studied, we knew that our fluid had a yield stress behavior under the action of the electric field. The characterization of yield stress fluids under uniaxial extensional flow had been previously reported by [18,21,29,30]. It is well accepted in the literature that the filament will begin the thinning process once the capillary pressure ($2\sigma/D_{min}$) is greater than the dynamic yield stress (τ_{yd}). Although Bingham's model is not accurate for predicting the temporal variation of the minimum filament diameter [21], it is able to predict the yielding diameter (Equation (3)) very accurately: [13]:

$$D_y = \frac{2\sigma}{\tau_{yd}\sqrt{3}}, \tag{3}$$

where σ is the surface tension and τ_{yd} the dynamic yield stress. The yielding diameter is defined as the threshold diameter necessary to cross in order to start the thinning process; thus:

- if $D_y > d_f$, being $d_f \approx d_0\sqrt{h_0/h_f}$, the capillary pressure exceeds the dynamic yield stress, and the filament thinning will be triggered;
- if $D_y < d_f$, the capillary pressure does not exceed the dynamic yield stress, and the thinning process will not begin, so the filament will not break;

where d_f is the filament diameter at the end of the step strain deformation.

The results from the extensional electrorheometry of the cornstarch suspension are shown in Figure 8, where the effect of the intensity of the electric field and its polarity becomes evident. In the absence of the electric field, the minimum diameter of the filament corresponding to the ERF followed a similar evolution to the one of the carrier fluid, as both showed Newtonian behavior. As the intensity

of the electric field increased, the internal structure developed by the cornstarch particles helped the filament to counterbalance the capillary pressure, and consequently, the filament lived longer. There was a critical intensity of the electric field ($E_{0,cr}$) beyond which the filament became stable, and it did Not Break (NB), which can be observed by the fact that the diameter of the filament reached a constant value (Figure 8). The dynamic yield stress increased with the imposed electric field; therefore, if the capillary force after step strain did not exceed that value of dynamic yield stress, the filament thinning process did not begin, and the liquid bridge remained stable, bridging the h_f distance between the two plates. As stated above, if the diameter of the filament at the end of the streak time (d_f) was greater than the yielding diameter (D_y), then the capillary pressure did not exceed the dynamic yield stress, and the thinning process could not start. Table 4 presents the comparison between the diameter at the end of the streak time and the yielding diameter for all cases studied. According to the criteria of $d_f < D_y$, the filament should stop breaking for intensities of electric field $E_{0,cr} \geq 1.125$ kV/mm; however, results showed that an inverse polarity helped in the stabilization of the liquid bridge, and less intensity of the electric field was therefore required.

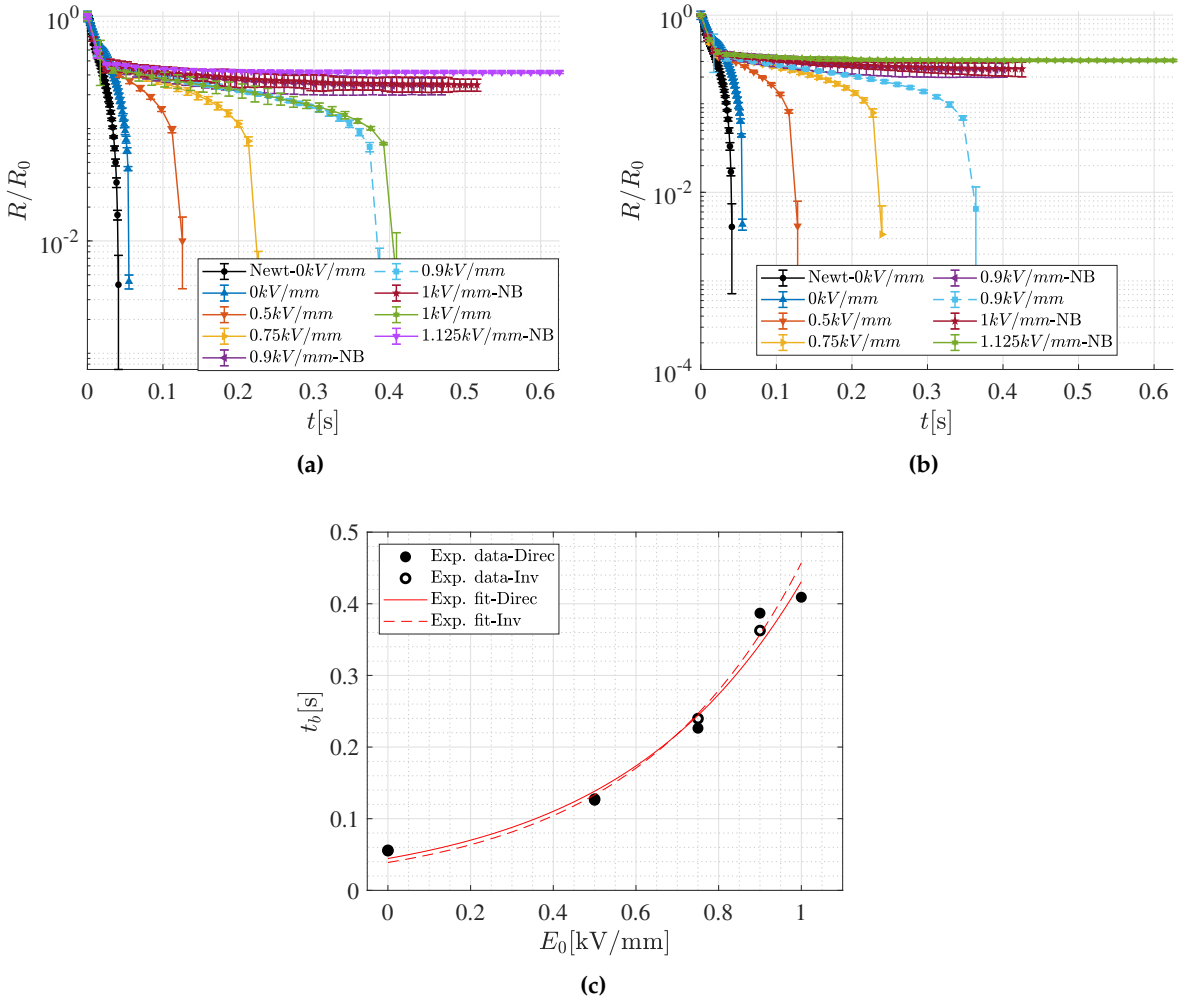

Figure 8. Effect of the electric field ($E = \Delta V/h_f$) on the cornstarch suspension on direct polarity (**a**) and inverse polarity (**b**) in all cases; for the sake of clarity, these experimental curves only show one out of 10 points.. (**c**) Exponential relation of the break time ($t_b\,(E_0) = A \cdot e^{b \cdot E_0}$, with E_0 in kV/mm), where the fitting parameters are provided in Table 6.

Table 4. d_f vs. D_y for each extensional electric field value. NB, Not Break.

wt.%	d_f	$E_0 = \frac{\Delta V}{h_0}$	$D_y = \frac{2\sigma}{\tau_{yd}\sqrt{3}}$	Direct	Inverse
30	2,25	0.5	9.284	B	B
		0.75	5.86	B	B
		0.9	2.96	B and NB	B and NB
		1	2.60	B and NB	NB
		1.125	2.08	NB	NB
		1.25	1.76	NB	NB
		1.5	1.17	NB	NB

However, the experimental results showed that in the case of the direct polarity, $E_{0,cr}$ was somewhere between 0.75 and 1.125 kV/mm (Figure 8a), while in the case of the inverse polarity, the critical value was between 0.75 and 1 kV/mm (Figure 8b). This result is consistent with the one obtained for the Newtonian case, where we could see that in the inverse polarity, the Coulomb-type forces could counterbalance the effect of the gravitational force and provide a longer filament life. Now, in the case of the ERF, the inverse polarity helped to create stable liquid bridges at a lower electric field.

Experimentally, it was not possible to extract the exact value of $E_{0,cr}$, but a transition zone. This was due to the fact that the used fluid model was not monodisperse in particle size (see Figure 1a). Table 5 establishes some indicative limits for the transition zone based on the cases studied in this research.

Table 5. Estimated limits of the transition zone: direct and inverse polarity.

Polarity	E Limits (kV/mm)
Direct	[0.75< E_0 <1.125]
Inverse	[0.75< E_0 <1]

The imposed electric field allowed the cornstarch particles to form chains aligned in the direction of the field, producing a slow down in the thinning process. The greater the number of elements in the chains or the number of chains, due to an increase in the electric field, the greater the viscosity of the fluid and, therefore, the longer the filament break-time (t_b). In Figure 8c, it can be observed that the break-time increased exponentially with respect to the applied electric field (E_0). The polarity had almost no effect at low intensities of the electric field ($E_0 < 0.5$ kV/mm); however, at higher electric field values, the break up time tended to be larger with the inverse polarity (Table 6).

Table 6. Dependence of the break time with the applied electric field and polarity ($t_b\,(E_0) = A \cdot e^{b \cdot E_0}$, with E_0 in kV/mm) for the cornstarch/olive suspension.

Polarity	A	B	R^2
Direct%	0.045	2.27	0.97
Inverse%	0.040	2.46	0.99

Figure 9 shows the time evolution of the minimum diameter for the working fluids under different electric fields. It could be observed that below a critical intensity of the electric field, the polarity had no effect on the thinning process of the filament, with the curves overlapping for both the Newtonian and the ERF fluids (Figure 9a). However, above a critical value of the intensity of the applied electric field (Figure 9b), the polarity had a clear effect on the time evolution of the minimum diameter for the ERF; for the Newtonian fluids, due to the absence of cornstarch particles, a much larger intensity of the electric field was required to see the influence of the polarity, i.e., Coulomb forces, as shown in Figure 5.

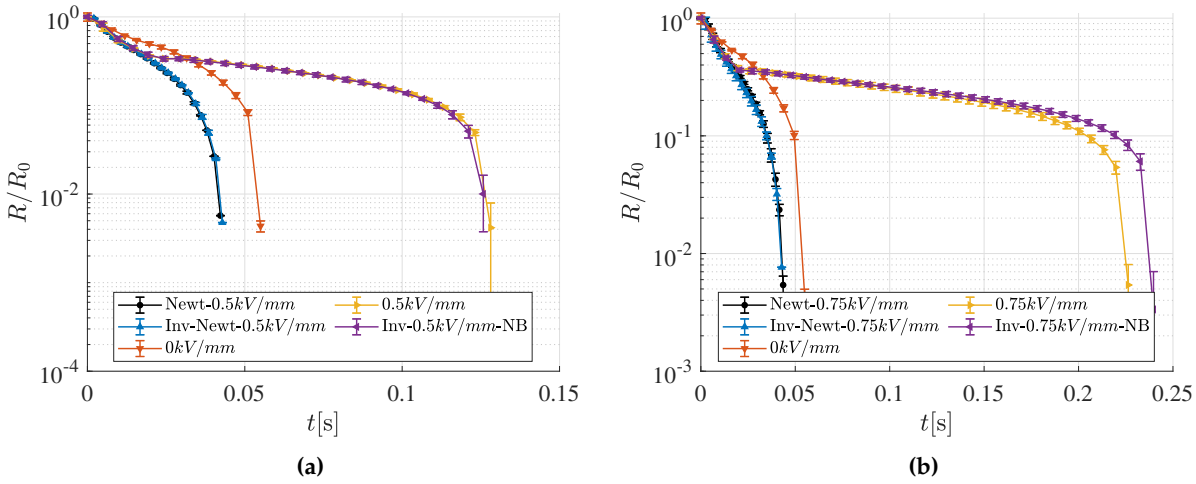

Figure 9. Effect of the polarity on the time evolution of the minimum diameter at (**a**) $E_0 = 0.5$ kV/mm and (**b**) $E = 0.75$ kV/mm. For the sake of clarity, each experimental curve only shows one out of 10 points.

4. Conclusions and Final Remarks

The novel ERD developed by Sadek et al. [13] for the CaBER opened a new door for the characterization of electrorheological properties of the ERFs under extensional flow. This electrorheological cell imposes an electric field aligned in the direction of the flow, which is also aligned with the gravitational force. Therefore, it was relevant to analyze the influence of the polarity in the electric field on the results obtained with this device.

The working fluids of this research work consisted of a Newtonian fluid (extra virgin olive oil) and an electrorheological fluid (concentrated suspension of cornstarch in extra virgin olive oil). Despite that the shear flow measurements revealed no influence of the electric field on the measurements, the results from the CaBEER experiments showed that the electric field had an effect on the thinning process of the olive oil, which depended on the polarity. This discrepancy in the results could be explained based on both the alignment of the electric and flow fields and the presence of Coulombian-type forces that probably came either from the impurities of the olive oil or from the inevitable electrochemical reactions at the metal-electrode/liquid interface, which, in the case of the direct configuration, would help the gravitational force to break the filament in a shorter time than the Newtonian case; in opposition to the inverse case, where the Coulombian forces counterbalanced the gravitational force and allowed the filament of the olive oil to live longer.

In the case of the electrorheological fluid, it was confirmed that having a yield diameter (D_y) smaller than the diameter of the filament at the end of the step strain deformation (d_f) ensured a stable filament that would never break while the electric field was active throughout the fluid sample. However, it was found that there was a transition zone between non-stable and stable filaments. That transition zone was found to be wider for the direct polarity. Additionally, it was found that having an inverse polarity in the experiments helped to generate more stable liquid bridges that would not break even if $d_f < D_y$.

New experiments with a better model fluid combined with numerical simulations will be helpful to gain deeper insight into the physics of this problem. We hope that this manuscript motivates and inspires the researchers in the field to further study this topic in the future.

Supplementary Materials: The following is available online at http://www.mdpi.com/2076-3417/9/24/5273/s1, Video S1: video1_inv_500fps.avi; Video S2: video1_direc_500fps.avi. Video S1—Video showing the time evolution of the minimum radius for the Newtonian fluid at h_0; no step strain was applied, just the electric field with the inverse polarity (Figure 6b—top row). Video S2—Video showing the time evolution of the minimum radius for the Newtonian fluid at h_0; no step strain was applied, just the electric field with the direct polarity (Figure 6b—bottom row).

Author Contributions: Conceptualization, J.H.G.-O. and F.J.G.-R.; methodology, J.H.G.-O., S.H.S., and F.J.G.-R.; software, J.H.G.-O.; validation, J.H.G.-O. and F.J.G.-R.; formal analysis, J.H.G.-O. and F.J.G.-R.; writing, original draft preparation, J.H.G.-O.; writing, review and editing, F.J.G.-R. and S.H.S.; supervision, F.J.G.-R.; project administration, F.J.G.-R.; funding acquisition, F.J.G.-R. and J.H.G.-O.

Funding: This research was funded by Programa de Fomento e impulso de la actividad investigadora de la Universidad de Cádiz 2018/19 and Fundação para a Ciência e a Tecnologia (FCT), COMPETE, and FEDER through projects MIT-EXPL/IRA/0077/2017 (FERRO-CLEAN) and POCI-01-0145-FEDER-030765 (RheoOptimized2DInks).

Acknowledgments: F.J.G.R. acknowledges the financial support provided by Fundação para a Ciência e a Tecnologia (FCT), COMPETE, and FEDER through projects MIT-EXPL/IRA/0077/2017 (FERRO-CLEAN) and POCI-01-0145-FEDER-030765 (RheoOptimized2DInks). J.H.G.-O. also acknowledges "Programa de Fomento e impulso de la actividad investigadora de la Universidad de Cádiz 2018/19".

Conflicts of Interest: The funders had no role in the design of the study; in the collection, analyzes, or interpretation of data; in the writing of the manuscript; nor in the decision to publish the results.

Abbreviations

The following abbreviations are used in this manuscript:

CaBER	Capillary Breakup Extensional Rheometer
CaBEER	Capillary Breakup Extensional Electrorheometry
ERD	Electrorheological Device
ExERF	Extensional Electrorheological Fixture

References

1. Winslow, W. Method and Means for Translating Electrical Impulses into Mechanical Force. U.S. Patent 2417850, 25 March 1947.
2. Winslow, W.M. Induced Fibration of Suspensions. *J. Appl. Phys.* **1949**, *20*, 1137–1140. [CrossRef]
3. Block, H.; Kelly, J.P. Electro-rheology. *J. Phys. D Appl. Phys.* **1988**, *21*, 1661–1677. [CrossRef]
4. Barnes, H.A.; Hutton, J.F.; Walters, K. *An Introduction to Rheology*; Rheology Series; Elsevier Science Publishers B.V.: Holanda, The Netherlands, 1993; Volume 3.
5. Galindo-Rosales, F.J. Complex Fluids and Rheometry in Microfluidics. In *Complex Fluid-Flows in Microfluidics*; Galindo-Rosales, F.J., Ed.; Springer: Cham, Switzerland, 2018; pp. 1–23. [CrossRef]
6. Gast, A.P.; Zukoski, C.F. Electrorheological fluids as colloidal suspensions. *Adv. Colloid Interface Sci.* **1989**, *30*, 153–202. [CrossRef]
7. Halsey, T.C.; Toor, W. Structure of electrorheological fluids. *Phys. Rev. Lett.* **1990**, *65*, 2820–2823. [CrossRef]
8. Sheng, P.; Wen, W. Electrorheological Fluids: Mechanisms, Dynamics, and Microfluidics Applications. *Annu. Rev. Fluid Mech.* **2012**, *44*, 143–174. [CrossRef]
9. Stanway, R.; Sproston, J.; Prendergast, M.; Case, J.; Wilne, C. ER fluids in the squeeze-flow mode: An application to vibration isolation. *J. Electrost.* **1992**, *28*, 89–94. [CrossRef]
10. Engmann, J.; Servais, C.; Burbidge, A.S. Squeeze flow theory and applications to rheometry: A review. *J. Non-Newton. Fluid Mech.* **2005**, *132*, 1–27. [CrossRef]
11. Haward, S.J.; Jaishankar, A.; Oliveira, M.S.N.; Alves, M.A.; McKinley, G.H. Extensional Flow of Hyaluronic Acid Solutions in an Optimized Microfluidic Cross-Slot Device. *Biomicrofluidics* **2013**, *7*, 044108. [CrossRef]
12. Galindo-Rosales, F.J.; Alves, M.A.; Oliveira, M.S.N. Microdevices for extensional rheometry of low viscosity elastic liquids: A review. *Microfluid. Nanofluid.* **2013**, *14*, 1–19. [CrossRef]
13. Sadek, S.; Najafabadi, H.; Galindo-Rosales, F. Capillary Breakup Extensional ElectroRheometry (CaBEER). *J. Rheol.* **2020**, *64*, 43. [CrossRef]
14. Sadek, S.; Najafabadi, H.; Campo-Deaño, L.; Galindo-Rosales, F. Extensional Magneto-Rheological Fixture (ExMRFx). Patent No. 20191000020360 COD 0198, 12 April 2019.

15. Akbari, A.; Hill, R.J. Liquid-bridge stability and breakup on surfaces with contact-angle hysteresis. *Soft Matter* **2016**, *12*, 6868–6882. [CrossRef] [PubMed]
16. Dinkgreve, M.; Denn, M.M.; Bonn, D. "Everything flows?": Elastic effects on startup flows of yield-stress fluids. *Rheol. Acta* **2017**, *56*, 189–194. [CrossRef]
17. McKinley, G.H.; Tripathi, A. How to Extract the Newtonian Viscosity from Capillary Breakup Measurements In a Filament Rheometer. *J. Rheol.* **2000**, *44*, 653–671. [CrossRef]
18. McKinley, G.H. *Visco-Elasto-Capillary Thinning and Break-Up of Complex Fluids*; Rheology Reviews; The British Society of Rheology: Malvern, UK, 2005; Volume 3, pp. 1–48.
19. Yao, M.; McKinley, G.H. Numerical Simulation of Extensional Deformations of Viscoelastic Liquid Bridges in Filament Stretching Devices. *J. Non-Newton. Fluid Mech.* **1998**, *74*, 47–88. [CrossRef]
20. Galindo-Rosales, F.J.; Segovia-Gutiérrez, J.P.; Pinho, F.T.; Alves, M.A.; de Vicente, J. Extensional rheometry of magnetic dispersions. *J. Rheol.* **2015**, *59*, 193–209. [CrossRef]
21. Niedzwiedz, K.; Arnolds, O.; Willembacher, N.; Brummer, R. How to Characterize Yield Stress Fluids with Capillary Breakup Extensional Rheometry (CaBER)? *Appl. Rheol.* **2009**, *19*, 41969. [CrossRef]
22. Campo-Deaño, L.; Clasen, C. The slow retraction method (SRM) for the determination of ultra-short relaxation times in capillary breakup extensional rheometry experiments. *J. Non-Newton. Fluid Mech.* **2010**, *165*, 1688–1699. [CrossRef]
23. Najafabadi, H.; Sadek, S.; Campo-Deaño, L.; Galindo-Rosales, F. Time Effect in Extensional Electrorheological Characterization. In *Recent Developments in Rheology (IBEREO2019)*; Galindo-Rosales, F., Campo-Deaño, L., Afonso, A., Alves, M., Pinho, F., Eds.; Springer: Cham, Switzerland, 2019; pp. 152–156. [CrossRef]
24. Paranjpe, G.R.; Deshpande, P.Y. Dielectric properties of some vegetable oils. *Proc. Indian Acad. Sci. Sect. A* **1935**, *1*, 880–886. [CrossRef]
25. Conrad, H.; Li, Y.; Chen, Y. The temperature dependence of the electrorheology and related electrical properties of cornstarch/corn oil suspensions. *J. Rheol.* **1995**, *39*, 1041–1057. [CrossRef]
26. González, H.; Mccluskey, F.M.J.; Castellanos, A.; Barrero, A. Stabilization of dielectric liquid bridges by electric fields in the absence of gravity. *J. Fluid Mech.* **1989**, *206*, 545–561. [CrossRef]
27. Parthasarathy, M.; Klingenberg, D.J. Electrorheology: Mechanisms and models. *Mater. Sci. Eng. R Rep.* **1996**, *17*, 57–103. [CrossRef]
28. Davis, L.C.; Ginder, J.M. Electrostatic Forces in Electrorheological Fluids. In *Progress in Electrorheology: Science and Technology of Electrorheological Materials*; Havelka, K.O., Filisko, F.E., Eds.; Springer: Boston, MA, USA, 1995; pp. 107–114. [CrossRef]
29. Niedzwiedz, K.; Buggisch, H.; Willembacher, N. Extensional rheology of concentrated emulsions as probed by capillary breakup elongational rheometry (CaBER). *Rheol. Acta* **2010**, *49*, 1103–1116. [CrossRef]
30. Martinie, L.; Buggisch, H.; Willenbacher, N. Apparent elongational yield stress of soft matter. *J. Rheol.* **2013**, *57*, 627–646. [CrossRef]